Cell, Vol. 100, 301–309, February 4, 2000, Copyright ©2000 by Cell Press

Large-Scale Movement of Elongation Factor G and Extensive Conformational Change of the Ribosome during Translocation

Holger Stark,*§ Marina V. Rodnina,† Hans-Joachim Wieden,† Marin van Heel,* and Wolfgang Wintermeyer†‡
*Imperial College of Science
Medicine and Technology
Department of Biochemistry
London SW7 2AY
United Kingdom
†Institut für Molekularbiologie
Universität Witten/Herdecke
58448 Witten
Germany

Summary

Elongation factor (EF) G promotes tRNA translocation on the ribosome. We present three-dimensional reconstructions, obtained by cryo–electron microscopy, of EF-G-ribosome complexes before and after translocation. In the pretranslocation state, domain 1 of EF-G interacts with the L7/12 stalk on the 50S subunit, while domain 4 contacts the shoulder of the 30S subunit in the region where protein S4 is located. During translocation, EF-G experiences an extensive reorientation, such that, after translocation, domain 4 reaches into the decoding center. The factor assumes different conformations before and after translocation. The structure of the ribosome is changed substantially in the pretranslocation state, in particular at the head-to-body junction in the 30S subunit, suggesting a possible mechanism of translocation.

Introduction

The translocation step in the protein elongation cycle entails a large-scale rearrangement in which two mRNA-bound tRNAs move from their pre- to their posttranslocation sites on the ribosome. The process is promoted by elongation factor G (EF-G), a member of the GTPase superfamily. Thus far, the mechanism of translocation catalysis by EF-G and the role of GTP hydrolysis has not been understood. While translocation takes place slowly with nonhydrolyzable GTP analogs or, very slowly, even without EF-G (Spirin, 1985), the presence of the factor and GTP hydrolysis is essential for the reaction to take place rapidly (Rodnina et al., 1997). It is likely that GTP hydrolysis and/or the subsequent dissociation of inorganic phosphate induce conformational strain in EF-G, which, in turn, is coupled to a structural change of the ribosome that allows, or promotes, the movement of the tRNAs (Rodnina et al., 1997). The presumed structural change of EF-G is hypothetical, as only the structures of EF-G·GDP (Czworkowski et al., 1994; Al-Karadaghi et al., 1996) and of nucleotide-free EF-G (Ævarsson et al., 1994) are known. Changes of the ribosome structure related to translocation were postulated (Spirin, 1985) but not demonstrated experimentally. The comparison of pre- and posttranslocation ribosome-tRNA complexes by cryo–electron microscopy did not reveal significant differences in the structure of the ribosome or in the arrangement of the subunits relative to each other (Stark et al., 1997a).

To understand the mechanism of EF-G function on the ribosome, the complexes of ribosomes with EF-G have to be characterized structurally. The electron microscopic reconstruction of an EF-G-ribosome complex formed in the presence of fusidic acid placed EF-G such that domain 5 appears to contact the base of the stalk and domain 4 reaches into the cleft of the 30S subunit at or near the decoding center, while the G domain (domain 1) is involved in an interaction with a structural element extending from the L7/12 stalk (Agrawal et al., 1998). The arrangement was found to be similar in posttranslocation complexes containing tRNA and EF-G with either GDP and fusidic acid or EF-G with a nonhydrolyzable GTP analog (Agrawal et al., 1999), while the pretranslocation position of EF-G could not be defined. A similar posttranslocation arrangement of EF-G was derived from hydroxyl radical cleavages in both 16S and 23S rRNA directed from Fe^{2+}-EDTA tethered to various surface positions of EF-G (Wilson and Noller, 1998). Data from cross-linking (Sköld, 1983), chemical footprinting (Moazed et al., 1988), and functional assays (Hausner et al., 1987) defined EF-G-ribosome interaction sites at the sarcin-ricin stem–loop (SRL) around residue 2660 of 23S rRNA and at the L11 binding site around residue 1070 of 23S rRNA. The respective isolated RNA stem–loops were shown to form complexes with EF-G (Munishkin and Wool, 1997).

The structural information on EF-G-ribosome complexes referred to above defined the posttranslocation state of EF-G on the ribosome, which in most studies was stabilized by fusidic acid. Studying EF-G-ribosome complexes in the pretranslocation state proved difficult, mainly because translocation takes place rapidly after binding of EF-G to the pretranslocation ribosome, even when GTP is replaced with nonhydrolyzable analogs (Rodnina et al., 1997). Taking advantage of the inhibition by thiostrepton of both translocation and EF-G turnover observed recently (Rodnina et al., 1999), we were able to freeze EF-G-ribosome complexes in both pre- and posttranslocation states and to study them by cryo–electron microscopy.

We report three-dimensional reconstructions, at resolutions of 18–20 Å, of ribosome-tRNA-EF-G complexes in two states, that is, immediately before and after translocation. The position of EF-G in the final posttranslocation state stabilized by fusidic acid, as reported (Agrawal et al., 1998), was also determined for comparison. The implications of EF-G-induced structural changes of the

‡To whom correspondence should be addressed (e-mail: winterme@uni-wh.de).
§Present Address: Institut für Molekularbiologie und Tumorforschung, Philipps-Universität, 35037 Marburg, Germany.

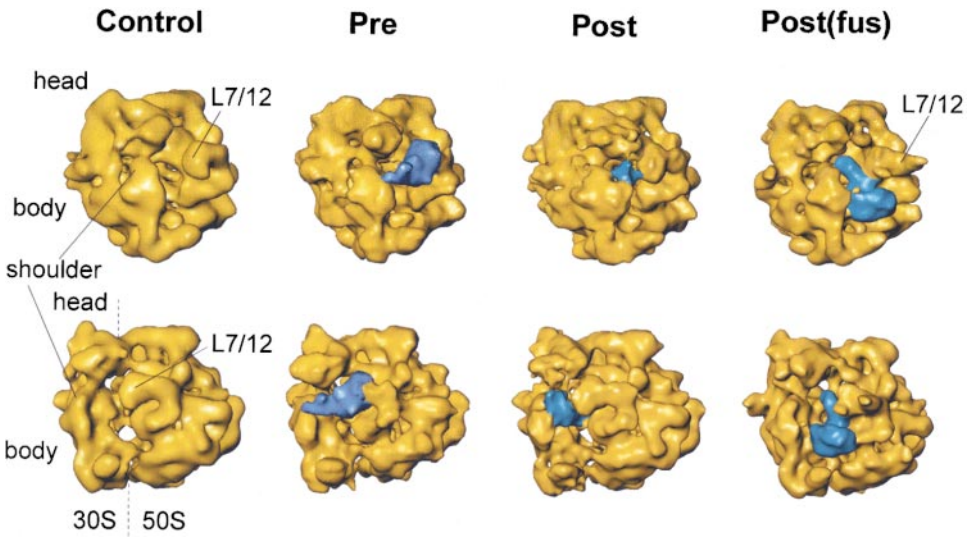

Figure 1. Three-Dimensional Reconstructions of Ribosome Complexes

Ribosomes are depicted with the 30S subunit to the left and the 50S subunit to the right in two views rotated by about 30°. Densities attributed to EF-G on the basis of difference densities (cf. Figure 2) are depicted in blue. Control, pretranslocation complex without EF-G; pre, pretranslocation complex with EF-G; post, posttranslocation complex with EF-G; post(fus), ribosome-EF-G complex formed in the presence of fusidic acid. For complex preparation and electron microscopy, see Experimental Procedures. L7/L12, proteins forming the stalk of the 50S subunit. Surface representations were prepared using the program Iris Explorer.

ribosome for the mechanism of translocation are discussed.

Results

Preparation of Pre- and Posttranslocation EF-G-Ribosome Complexes

Ribosomes in the pretranslocation state were prepared from 70S initiation complexes carrying fMet-tRNA^{fMet} in the P site by binding Phe-tRNA^{Phe} in a complex with EF-Tu·GTP to the A site; subsequent peptide bond formation yielded pretranslocation ribosomes with tRNA^{fMet} in the P site and fMet-Phe-tRNA^{Phe} in the A site. Complexes were studied in the states immediately preceding (pre) and following (post) the movement of the tRNAs. In the presence of thiostrepton, translocation is sufficiently slow to allow the EF-G-ribosome complex to be frozen in the pre state before the movement of the tRNAs has proceeded to any significant extent. On the other hand, by further incubating the complex prior to freezing, the post state with peptidyl-tRNA in the P site and bound EF-G·GDP can be obtained from the pre complex. Thus, the two complexes studied, pre and post, are identical biochemically, except that translocation has taken place. According to the biochemical analysis, at least 85% of the ribosomes were in the pre- or posttranslocation state, respectively (Experimental Procedures). The complex of EF-G in the posttranslocation position stabilized by fusidic acid on ribosomes without tRNAs, post(fus), was prepared as described (Experimental Procedures).

Arrangement of EF-G on the Ribosome before and after Translocation

Three-dimensional reconstructions of ribosome-EF-G complexes are shown in Figure 1 along with a control ribosome-tRNA complex without EF-G. Density attributable to EF-G is clearly identified in the three complexes. In the pre complex, density due to EF-G is seen bridging the cleft between the two subunits. The density emerges from the L7/12 stalk on the 50S subunit and contacts the shoulder of the 30S subunit at the bottom of a large cleft between head and shoulder of the 30S subunit. There are no other contacts of EF-G with the ribosome in the pre state.

The arrangement of EF-G in the post complex is entirely different. The comparison with the control complex now reveals additional density closely attached to the 30S subunit, indicating that the EF-G molecule has undergone a major movement into the intersubunit space. The strong connection of EF-G to L7/12 prevailing in the pre complex has been largely lost in the post complex, except for some density emerging from the globular head of the L7/12 stalk and forming a bridge to the density attributed to EF-G. Instead, there are several contacts between EF-G and both body and head of the 30S subunit.

In the post(fus) complex, the density due to EF-G is located in the intersubunit space and protrudes toward the outside of the ribosome. An extended structural element (domain 4, see below) is oriented toward the decoding center in the 30S subunit. Another prominent feature of this complex is the extended structure of the L7/12 stalk. In its main features, the present reconstruction of the post(fus) complex is similar to the previous reconstruction of the same complex reported by Agrawal et al. (1998); differences are discussed below.

Conformation of EF-G in Ribosomal Complexes

Density due to EF-G was identified as positive density in difference maps obtained by subtracting the density

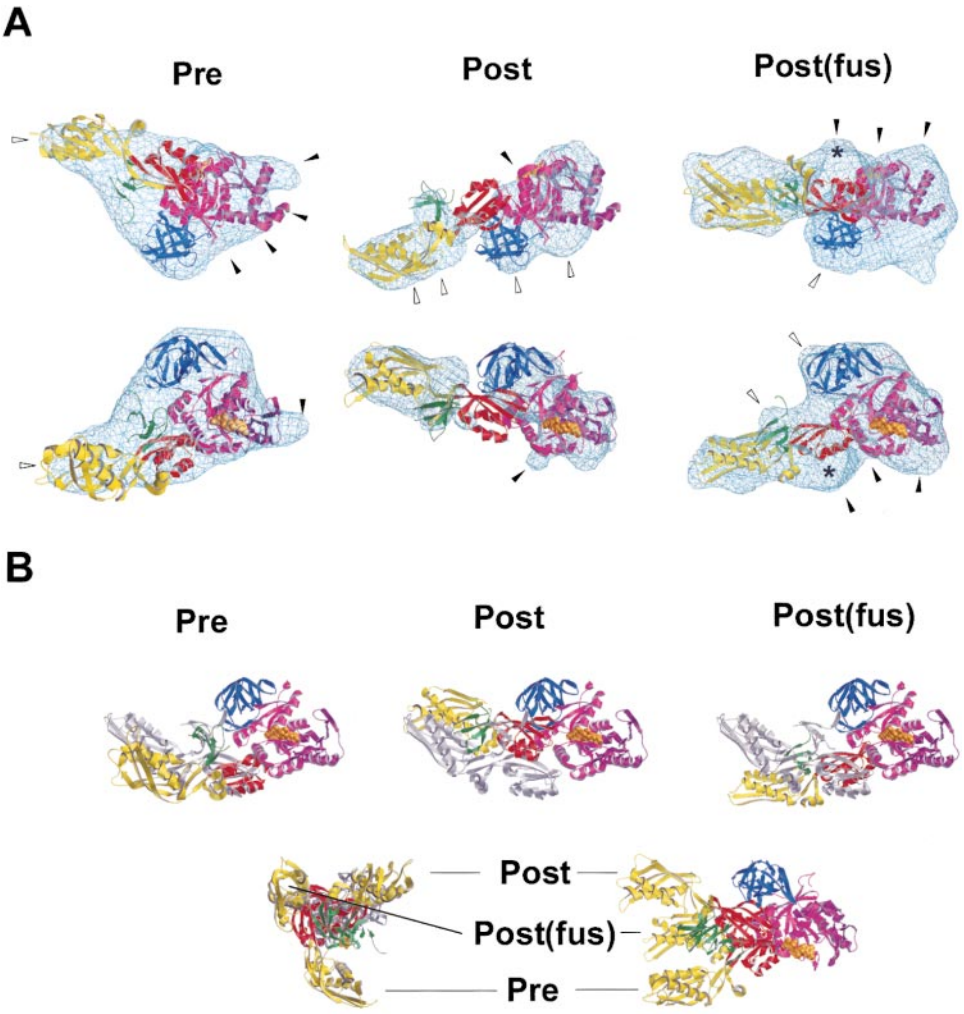

Figure 2. Arrangement and Conformation of EF-G on the Ribosome

(A) Orthogonal views of difference densities fitted with EF-G. Density attributed to EF-G was cut from difference maps obtained by subtracting the density of the respective control complexes from the density of pre, post, or post(fus) complexes. The structure of EF-G was fitted interactively to match the observed difference density, based on the crystal coordinates of EF-G·GDP (Czworkowski et al., 1994; Al-Karadaghi et al., 1996), but allowing for movements of domains 3/4/5 relative to domains 1/2. The accuracy of the fits is estimated to ± 10° for the rotational parameters and ± 3 Å for the translational parameters. Color code for EF-G domains: domain 1, magenta; domain 2, blue; domain 3 (only partially defined in the crystal structure), green; domain 4, yellow; domain 5, red. Ribosome contacts are indicated by open (30S) or closed (50S) arrowheads. Density due to the ribosome is marked by an asterisk.

(B) Conformations of EF-G. Top panels: Superpositions of the fitted EF-G structures and the crystal structure of EF-G. GDP (domains 4 and 5 of the latter are in gray), aligned on domains 1 and 2. Bottom panels: Overlay of the fitted EF-G structures in the three complexes studied, aligned on domains 1 and 2. Domain 5 (red) is present in three different positions not distinguished by color.

of the control complex from the densities of the pre and post complexes (Figure 2, top panels). Because the structures of these three complexes differ from that of the control in other parts of the ribosome (see below), difference densities not directly related to EF-G are omitted in Figure 2. The EF-G densities were interpreted by fitting the crystal structure of *Thermus thermophilus* EF-G·GDP (Ævarsson et al., 1994; Czworkowski et al., 1994). While the overall orientation of EF-G could be delineated by fitting the crystal structure, in none of the complexes did the observed density accommodate the crystal structure fully, indicating that EF-G on the ribosome assumes conformations that differ from that of EF-G·GDP in the crystal, as was reported previously for the ribosome-EF-G complex stabilized by fusidic acid (Agrawal et al., 1998). To approximate potential conformational changes of EF-G in the three complexes studied here, two parts of the EF-G molecule, comprising domains 1/2 and domains 3/4/5, respectively, were allowed to move relative to each other during the fitting.

The difference density representing EF-G was defined best in the ribosome-EF-G complex containing fusidic acid, post(fus); the quality of the map may reflect a restricted flexibility of the factor with bound antibiotic. The best fit to the density was obtained with a conformation of EF-G in which domain 5 is moved toward domain 2, resulting in a large (about 40 Å) displacement of the tip of domain 4 (Figures 2A and 2B, right panels). A few

ribosome contacts are also seen, including density that is not filled by EF-G and, based on the assignment of Ban et al. (1999), is attributed to the SRL. Both arrangement and conformation of EF-G in the post(fus) complex are similar to that described for the same complex by Agrawal et al. (1998).

In the pre complex (Figure 2A, left panels), the fit suggests an orientation of EF-G where domain 1 extensively interacts with the L7/12 stalk on the 50S subunit, while domain 4 reaches across the intersubunit space and contacts the shoulder of the 30S subunit. The conformation of EF-G in the pre complex seems to be slightly more open compared to the crystal structure (Figure 2B, left panels), the main change consisting in a movement of domain 4 by about 30 Å from its position in the crystal structure.

In the post complex, the density of EF-G appears in a different position and suggests a different conformation of the factor in comparison to the crystal structure (Figure 2, middle panels). In this conformation, domain 5 is displaced toward domain 2 in a way that results in a 45° rotation of domain 4 and a 25–30 Å displacement of the tip region. The fit suggests an arrangement in which the body of EF-G is involved in several contacts with the 30S subunit close to the head-to-body junction and domain 4 reaches into the decoding center and approaches the anticodon of the P site–bound peptidyl-tRNA (Figure 3) .

The densities observed for EF-G suggest that the factor assumes different conformations in the three ribosomal complexes, mainly by a movement of domains 3/4/5 relative to domains 1/2 (Figure 2B). Although only small movements of domain 5 relative to domains 1/2 were required to fit the density, the resulting movements of the tip region of domain 4 are quite extensive, due to the extended structure of the arm formed of domains 5 and 4. In some places, in particular at the G′ subdomain and at helices B, C, and D of domain 1, small parts of the EF-G models are not accommodated in the density. While this may be due to local flexibility, it may also indicate that there are additional conformational changes in EF-G not accounted for by the fitting approach used here.

The different arrangements of EF-G in the pre and post complexes are depicted by the models of Figure 3 where the density of EF-G is given as calculated from the pre and post conformations of Figure 2. The indicated positions of the tRNAs were obtained by fitting observed densities with the tRNA crystal structures. In the pre state, the contact of domain 4 with the shoulder of the 30S subunit is clearly seen, whereas in the post state, the tip of domain 4 reaches deeply into the decoding center, and, at the same time, the body of the factor molecule has moved from the 50S subunit toward the 30S subunit. Domains 1/2/4 are involved in several interactions with the 30S subunit, including a strong interaction of domain 1 with the shoulder, a bridge to the 30S body, and another bridge to the head; the contact with L7/12 is reduced to a bridge of density connecting the globular part of L7/12 with domain 1 of EF-G (cf. Figures 1 and 2). Except for the latter interaction, there are no contacts of EF-G with the 50S subunit in the post state.

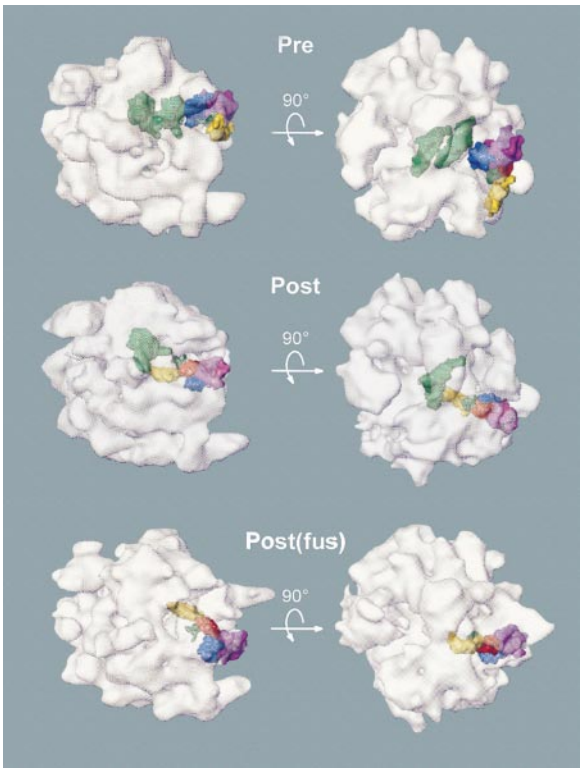

Figure 3. Orthogonal Views of the Arrangements of EF-G and tRNA in Ribosome Complexes

Ribosomes are depicted in transparent manner. Densities for EF-G (color-coded as in Figure 2) were calculated from the fits in Figure 2; tRNA densities (green) were calculated from the coordinates of the crystal structure of $tRNA^{Phe}$, filtered to a resolution of 10 Å, and were fitted into the observed density.

The tRNA positions in thiostrepton-containing complexes, compared to the previously studied ribosome-tRNA complexes without antibiotic (Stark et al., 1997a), appear somewhat different on the 50S subunit, while on the 30S subunit the respective positions are the same. This may indicate an influence of thiostrepton on the detailed positioning of the 3′ end of tRNA on the 50S subunit.

Structural Changes of the Ribosome Induced by EF-G

The structure of the ribosome, as viewed from the 30S solvent side, exhibits substantial structural differences at several characteristic landmarks of the small subunit when the pre complex is compared with the other complexes (Figure 4, top panels). Major differences are seen at the neck connecting head and body, at the connection between head and beak, and at the beak, which becomes more prominent. The latter change is also clearly seen in the side views of Figure 1, where in the pre complex the cleft or channel between the shoulder and the head of the 30S subunit is widened compared to the control or post complexes. The structure of the 50S subunit appears to be largely unchanged in the three complexes, except for the extended L7/12 stalk in the fusidic acid–stabilized complex (Figure 4).

In the pre complex, the relative arrangement of the

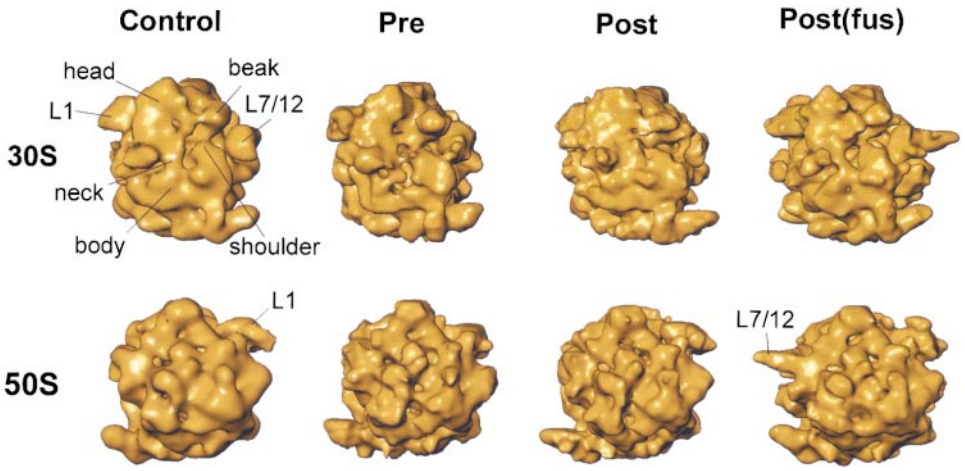

Figure 4. Conformations of the Ribosome

Three-dimensional reconstructions of EF-G-ribosome complexes viewed from the solvent side of 30S (upper panels) and 50S (lower panels) subunits.

subunits is not changed significantly compared to both the pretranslocation complex studied previously (Stark et al., 1997a) and the control pretranslocation complex containing thiostrepton studied here. In the post complex, the arrangement is slightly changed as the intersubunit space is opened on the side of the A site and closed on the side of the E site by 5° to 10°.

Comparison of the Arrangements of EF-G and EF-Tu on the Ribosome

The arrangement on the ribosome was compared with that of the kirromycin-stalled EF-Tu-aa-tRNA complex in the codon-recognition state (Stark et al., 1997b). In the latter complex, the anticodon arm reaches into the decoding center on the 30S subunit while EF-Tu is oriented toward the 50S subunit, contacting the base of the L7/12 stalk and the stalk itself. In the present pre complex, the arrangement of EF-G is perpendicular to that of the ternary complex, and EF-Tu and the body of EF-G occupy different positions on the 50S subunit (Figure 5). In particular, the position relative to the L7/12 stalk appears different, although there is an interaction between factor and L7/12 stalk in both complexes. In the post complex, the orientation of EF-G is roughly parallel to that of the ternary complex, with domain 4 pointing into the decoding center as the anticodon arm of the ternary complex, while the body of EF-G is in a position that differs from the one of EF-Tu. In the post(fus) complex, the position of EF-G almost coincides with that of the ternary complex in the codon-recognition complex.

Discussion

Large-Scale Reorientation of EF-G during Translocation

The comparison of the ribosome-EF-G complexes studied here reveal grossly different orientations of EF-G. In the pre state, the body of EF-G is oriented toward the 50S subunit, making extensive contact with the L7/12 stalk, while domain 4 reaches across the intersubunit cleft and interacts with the shoulder of the 30S subunit. In that region protein S4 was located by indirect methods (Capel et al., 1987; Powers and Noller, 1995) and, recently, by X-ray crystallography of 30S ribosomal subunits (Clemons et al., 1999). In the post state, domain 4 reaches into the decoding center at the position where the anticodon arm of the A site tRNA was bound prior

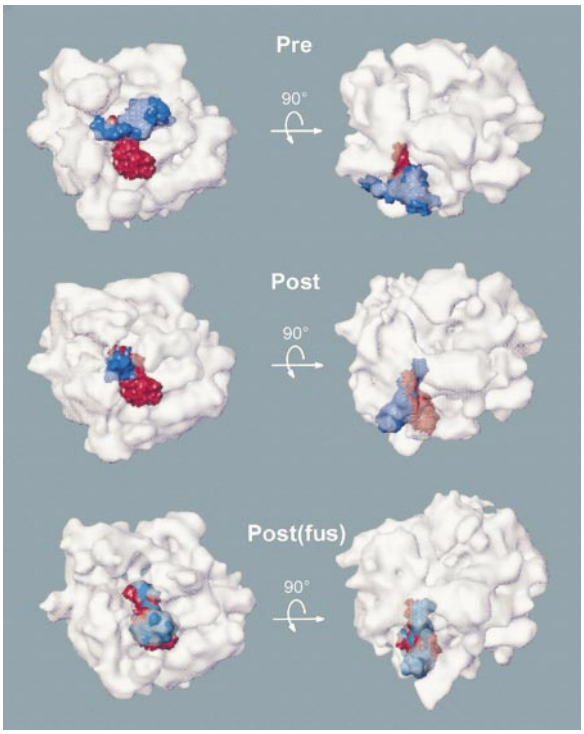

Figure 5. Comparison of the Positions of EF-G and EF-Tu-Phe-tRNA^{Phe} on the Ribosome

The position of EF-Tu-Phe-tRNA^{Phe} (red) was taken from the reconstruction of the kirromycin-stalled complex (Stark et al., 1997b) and placed into the reconstructions of the respective ribosome complexes with EF-G arranged as in Figure 3 (blue).

to translocation, while the body of EF-G interacts with the 30S subunit in the region of the head-to-body junction.

The gross orientation of EF-G in the post complex resembles the posttranslocational arrangement of the EF-G·GDP·fusidic acid complex on the ribosome in that domain 4 of EF-G is oriented toward the decoding center. There are, however, significant differences between the two complexes. In the reconstruction of the fusidic acid–stabilized complex, domains 1 and 5 of EF-G are oriented toward the 50S subunit and interact with the region at the base of the stalk in an arrangement similar to that described previously (Agrawal et al., 1998). The contact is likely to involve the SRL and the L11 binding region of 23S rRNA, as suggested by cleavages in the respective regions of 23S RNA caused by hydroxyl radicals originating from domains 1 and 5 (Wilson and Noller, 1998). The two regions of 23S rRNA are arranged close to each other in the 5 Å crystal structure of the 50S subunit (Ban et al., 1999). In contrast, in the reconstruction of the post complex containing thiostrepton, no contact of EF-G with the SRL is seen, in line with the lack of dimethyl sulphate footprints on the SRL (Rodnina et al., 1999). Thus, the two antibiotics appear to stabilize different states of the ribosome-EF-G complex, the thiostrepton-stabilized post state preceding the one stabilized by fusidic acid.

Domain 4 is important for the function of EF-G in translocation catalysis (Rodnina et al., 1997 and references therein). The positions on the ribosome of the aa-tRNA·EF-Tu complex in the codon-recognition complex stalled by kirromycin (Stark et al., 1997b) and of EF-G in the present post complex stabilized by thiostrepton are similar, but not identical. The positions overlap almost completely when the fusidic acid–stabilized ribosome-EF-G complex is compared (Figure 5), as has been noted before (Agrawal et al., 1998). This is in line with the "molecular mimicry" model that was based on the structural similarity of the EF-Tu·GTP·aa-tRNA complex and EF-G·GDP (Nissen et al., 1995). However, the parallel is restricted to the state after translocation, whereas in the pre state the orientation of EF-G on the ribosome is entirely different, and obviously has to be, because in the pretranslocation state domain 4 cannot reach into the 30S A site, which is occupied by peptidyl-tRNA.

Conformation of EF-G on the Ribosome

In order to optimally fit the densities observed for EF-G in the three ribosome complexes, pre, post, and post(fus), the structure of EF-G, as derived from the crystal structure of EF-G·GDP, had to be changed to different extents, indicating that the factor assumes different conformations in the three complexes studied. The best fits were obtained when the arrangement of domains 3/4/5 relative to domains 1/2 was changed, resulting in quite different positions of domain 4 in the three complexes. In all ribosome-EF-G complexes studied, the conformation of EF-G was different from that in the crystal structure of EF-G·GDP. For the posttranslocation states, this could be explained by an inhibition, by either thiostrepton (post) or fusidic acid (post(fus)), of the rearrangement toward the GDP-bound conformation of EF-G, in keeping with the fact that both antibiotics inhibit the dissociation of the factor from the ribosome. However, the two antibiotics affect different functional states by different mechanisms in that thiostrepton binds to 23S rRNA and is likely to interfere with a conformational change of the ribosome, whereas fusidic acid acts by binding to the factor.

Could the open conformation of EF-G in the pre complex represent the unknown GTP-bound conformation of EF-G? Following the binding of EF-G·GTP to the pretranslocation ribosome, GTP is hydrolyzed rapidly and the γ-phosphate is released within a few seconds in the presence of thiostrepton (Rodnina et al., 1999), suggesting that at the time when the complex was frozen for the analysis (about 1 min after complex formation), EF-G had only GDP bound to it. We speculate that the release of the γ-phosphate induces conformational strain in the molecule, which is used to drive the conformational change of the ribosome toward the state observed in the pre complex. The extent to which the conformation of EF-G changes during this transition is not known; thus, it remains open how closely the conformation of EF-G in the pre complex resembles the initial GTP-bound conformation.

EF-G-Induced Conformational Change of the Ribosome: the Mechanism of Translocation

The relative arrangement of the subunits is not significantly changed in the pre complex. Thus, at least in that state, there is no "unlocking" of the two subunits, which was suggested as a possible mechanism involved in translocation (Spirin, 1985). The structure of the 50S subunit is very similar in the pre and post complexes, whereas the 30S subunit in the pre state shows substantial structural differences compared to the pretranslocation ribosome without EF-G or to the post complex. The most significant changes in the 30S subunit are found in the region of the neck connecting body and head, in the head at the connection with the beak, and at the outer junction of head and shoulder, which is opened up significantly. The structure and relative orientation of these regions of the small subunit appear to be flexible, as a recent cryo–electron microscopic study of isolated 30S subunits has revealed structural variations mainly in these regions (Gabashvili et al., 1999).

The observed structural differences may be in part related to defined structural elements of the small subunit on the basis of a structural model of the 30S subunit (Mueller and Brimacombe, 1997a; 1997b) as well as of the recent 5.5 Å crystallographic structure of the 30S subunit (Clemons et al., 1999). According to those models, helix 34 of 16S rRNA is located in the head and is involved in a contact with the body. Thus, the structural changes observed in that region suggest that the arrangement of helix 34 is changed in the pre complex, leading to a widening of the gap between head and shoulder. Helix 34 is linked to translocation, as mutations at C1092 confer resistance to the antibiotic spectinomycin, an inhibitor of EF-G function (Sigmund et al., 1984; Bilgin et al., 1990), and it has been suggested that binding of spectinomycin stabilizes a particular conformation of helix 34, thereby inhibiting a functionally important conformational transition (Brink et al., 1994). The structural difference between the pre and the control complexes may well represent that transition.

The question remains how EF-G induces the particular structure of the 30S subunit in the pre complex. EF-G interacts with both subunits of the ribosome, contacting L7/12 on the large subunit and the S4 binding region at the shoulder of the small subunit. Hence, the 30S structure may be affected either directly or indirectly via the 50S subunit. Since the structure of the 50S subunit is not changed much in the pre complex, the latter possibility seems less likely. We propose, therefore, that the effect of EF-G is direct and that binding of domain 4 in the S4 region induces a structural change in the shoulder region that, in turn, brings about the structural changes observed at the neck and at the site of head and body interaction. One possibility is that the conformational change is propagated through 16S rRNA. S4 has been mapped to 16S rRNA at the junction of five helical elements (Heilek et al., 1995; Powers and Noller, 1995) of which one comprises helix 18 (530 loop) of 16S rRNA, a region known to be involved in a pseudoknot and to be crucially important for ribosome function (Powers and Noller, 1991; O'Connor et al., 1995). The 530 loop is oriented toward helix 34 (Noller et al., 1995; Mueller and Brimacombe, 1997a) and is conformationally coupled to the decoding region of 16S rRNA (Moazed and Noller, 1986; Powers and Noller, 1991). Motion at the S4 binding region may induce a conformational switch of the 530 pseudoknot structure, which may affect the interaction of the 530 stem–loop with helix 34, thereby changing the arrangement of the head relative to the body. In the latter change, protein S5 may also be involved, since it is situated close to protein S4 (Capel et al., 1987; Mueller and Brimacombe, 1997b) and, by its N-terminal domain, is oriented toward helix 34 in the head (Heilek et al., 1995), possibly making a contact there (Ramakrishnan and White, 1992; Davies et al., 1998).

Another region of the 30S subunit that is involved in translocation is the decoding center. There are numerous observations that relate structural changes of the decoding center, or their inhibition, to translocation. It has been reported that aminoglycoside antibiotics that bind to the decoding region on 16S rRNA and affect the fidelity of decoding also inhibit translocation (Davies and Davis, 1968). The antibiotic viomycin, which specifically inhibits translocation (Modolell and Vazquez, 1977), strongly protects position A1408 in the decoding center of 16S rRNA against chemical modification (Powers and Noller, 1994), in addition to protecting positions 913/914 in 23S rRNA (Moazed and Noller, 1987). In the pretranslocation state, the mRNA-tRNA complex interacts with 16S rRNA in the decoding center (VanLoock et al., 1999 and references therein). These interactions have to be released in order to allow the movement of the mRNA-tRNA complex independent of the 16S rRNA. The required conformational change of the decoding region of 16S rRNA may also involve a conformational switch in the 900 region (Lodmell and Dahlberg, 1997), which in the three-dimensional structure is located next to the decoding center (Cate et al., 1999; Clemons et al., 1999) and at the intersubunit interface (Cate et al., 1999).

It is possible that the formation of the transition state structure of the ribosome is sufficient for the movement of the tRNAs to take place, in line with the observation of spontaneous, slow translocation in the absence of EF-G (Spirin, 1985). In such a case, EF-G accelerates translocation by promoting the structural change of the ribosome toward the transition state, and tRNA movement as such is thermodynamically favored and spontaneous. However, alternative models in which the tRNA-mRNA movement is directly coupled to the conformational change of EF-G or of the ribosome are not excluded.

Interaction of EF-G with the L7/12 Stalk

EF-G interacts with the L7/12 stalk on the 50S subunit in both pre and post complexes. In the pre complex, the interaction is quite extensive and clearly involves domain 1 of EF-G; on the side of L7/12, the outer globular part of the stalk takes part in the interaction. In the post complex, the interaction is reduced to a small bridge of density connecting the outer part of the stalk with the body of EF-G. A connection between L7/12 and the factor was also observed in a ribosome-EF-Tu complex studied previously (Stark et al., 1997b), indicating that the contact with L7/12 is common for the elongation factors and may be functional. In fact, the presence of at least one copy of the L7/12 dimer on the ribosome has been shown to be essential for elongation factor function on the ribosome (Oleinikov et al., 1998), and recent results demonstrate that L7/12 strongly stimulates the GTPase activity of EF-G (Savelsbergh et al., 2000). The intimate contact of the L7/12 stalk with the body of EF-G observed in the pre complex probably reflects that functional interaction.

In the post(fus) complex, the L7/12 stalk, or a part of it, appears as an extended structure pointing away from the ribosome. The density of the extended structure is not very well defined and smears out in the map, indicating structural flexibility. An extended stalk in that complex was also reported by Agrawal et al. (1998), although in their reconstruction the stalk appears in a peculiar split structure that we have not observed. In the ribosome-EF-G complexes that contained tRNA, pre and post, we have not observed the extended, or bifurcated (Agrawal et al., 1999), forms of the stalk. The functional significance of the different forms of the stalk remains to be established.

Experimental Procedures

Ribosome Complexes

70S ribosomes from *E. coli* MRE 600 and EF-Tu from *E. coli* K12 were prepared as described (Rodnina and Wintermeyer, 1995). EF-G was expressed in *E. coli* JM109 from plasmid pTZ*fus* (Borowski et al., 1996). Cells were lysed with lysozyme (5 mg/g of wet cells) in buffer A (50 mM Tris HCl, pH 7.5, 10 mM $MgCl_2$, 0.5 mM EDTA, 6 mM β-mercaptoethanol) in the presence of 100 μM PMSF and 30 μM GDP, sodium deoxycholate (12.5 mg/g cells), and DNAse I (5 mg/g). The first purification step was chromatography on Sepharose CL6B (Pharmacia) using a 0–0.35 M KCl gradient in buffer A. Fractions containing EF-G were further purified by gel filtration on Superdex 75 HiLoad (Pharmacia) using buffer A containing 10% glycerol and 100 μM PMSF, and, subsequently, anion exchange chromatography on MonoQ (Pharmacia) using a 0–0.35 M KCl gradient in buffer A with 10% glycerol. EF-G was concentrated and stored in buffer B (50 mM Tris HCl, pH 7.5, 70 mM NH_4Cl, 30 mM KCl, 7 mM $MgCl_2$, 1 mM DTT) with 50% glycerol.

Initiation factors were isolated from overproducing strains provided by C. Gualerzi, University of Camerino, Italy. Cells were opened as above, using buffer C (20 mM Tris HCl, pH 7.7, 60 mM NH_4Cl, 10

mM $MgCl_2$, 5 mM β-mercaptoethanol, 0.1 mM PMSF). To wash initiation factors off the ribosomes, 1 M KCl was added to the S30 fraction, and after 10 min of incubation, the ribosomes were removed by centrifugation at 100,000 × g. From the supernatant, initiation factors were purified to homogeneity by Fast-Flow LC on S-Sepharose (Pharmacia) using a gradient of 0.2–0.8 M KCl in 50 mM MOPS, pH 6.4, 0.25 mM $MgCl_2$, 0.05 mM EDTA, 5 mM β-mercaptoethanol, 0.1 mM PMSF.

Ribosomes were programmed with MFTI-mRNA, which comprised 120 nucleotides and contained a ribosomal binding site and the coding sequence Met-Phe-Thr-Ile. The plasmid pXR022 coding for MFTI-mRNA (Calogero et al., 1988) was linearized by HindIII, and mRNA was prepared by run-off transcription with T7 RNA polymerase and purified by chromatography on MonoQ.

f[^{3}H]Met-tRNA^{fMet} was prepared as described (Rodnina et al., 1994). [^{14}C]Phe-tRNA^{Phe} from *E. coli* was purified by HPLC on RP18 (LiChrospher WP300, E. Merck, Darmstadt) using a gradient of 0% to 20% ethanol in 20 mM ammonium acetate, pH 5.5, 10 mM magnesium acetate, 0.4 M NaCl.

To prepare 70S initiation complexes, ribosomes (0.5 μM) were incubated with a 3-fold molar excess of MFTI-mRNA in the presence of a 1.5-fold excess each of IF1, IF2, IF3, and f[^{3}H]Met-tRNA^{fMet} in buffer B containing 1 mM GTP for 30 min at 37°C. Ternary complexes, EF-Tu·GTP·[^{14}C]Phe-tRNA^{Phe}, were prepared by incubating 1 μM EF-Tu with 1 mM GTP, 3 mM phosphoenol pyruvate, 0.5 mg/l pyruvate kinase, and 0.75 μM [^{14}C]Phe-tRNA^{Phe} in buffer B for 15 min at 37°C. Ternary complex was added to the initiation complex and incubated for 1 min at 37°C to form the pretranslocation complex. tRNA occupancy was 90% or better, as determined from ^{3}H and ^{14}C radioactivity on nitrocellulose filters, and peptide bond formation was quantitative according to peptide analysis by HPLC (Rodnina et al., 1997).

Equal volumes (20 μl each) of 0.5 μM pretranslocation complex and of 250 μM thiostrepton solution in 5% DMSO were mixed and incubated for 5 min at 37°C. EF-G (1.6 μM), preincubated with 1 mM GTP for 15 min at 37°C, was added to the pretranslocation complex in 10 μl and incubated further for 1 min at 20°C to obtain the pre complex. To prepare the post complex, the incubation with EF-G was continued for 45 min at 37°C. P site–bound fMetPhe-tRNA^{Phe} was determined by the puromycin assay (1 mM puromycin, 10 s at 37°C; [Rodnina et al., 1997]) and was below 5% and about 85% in the pre and post complexes, respectively.

Fusidic acid–stabilized complexes of ribosomes with EF-G·GDP were prepared by incubating vacant ribosomes (0.5 μM) with EF-G (2 μM) in the presence of GTP (1 mM) and fusidic acid (0.2 mM) in buffer B for 15 min at 37°C.

Electron–Cryo Microscopy and Image Processing

Solutions containing ribosome complexes (0.04 μM) were applied to holey carbon grids. After blotting the excess solution, the grid was rapidly plunged into liquid ethane leading to ribosome complexes embedded in a thin film of vitrified water spanning the holes on the carbon film. Electron micrographs were recorded under low dose conditions at liquid nitrogen temperature using a Gatan cryosystem in a Philips CM200 FEG cryo–electron microscope. Images at three different defocus values were recorded at a magnification of 66,000× in order to perform a complete correction of the phase contrast transfer function of the microscope.

Negatives were digitized on an EmiL CCD line-scanner (IMAGE Science GmbH) at a step size of 14 μm. The digitized images were binned by a factor of two resulting in a pixel size corresponding to 5 Å at the specimen level. Several thousands of individual molecules were interactively extracted (control complex: 3,100, pre: 6,400, post: 11,400, post(fus): 6,200 particles). After multireference alignment, multivariate statistical analysis, and automated hierarchical classification of the images, class averages of characteristic views were calculated with an improved signal-to-noise ratio. Subsequently, the Eulerian angles of these two-dimensional projection images were determined with the angular reconstitution approach (van Heel, 1987). Three-dimensional reconstructions were calculated by an exact filter backprojection algorithm (Harauz and van Heel, 1986). The entire sets of good class averages (~75% of all images) were used to obtain the final, completely CTF-corrected three-dimensional structures. The resolution of the three-dimensional structures was determined with the Fourier shell correlation function (FSC) (Harauz and van Heel, 1986) at a threshold of 3 σ with the following results: control complex, 20 Å; pre, 18 Å; post, 17 Å; post(fus), 20 Å.

Acknowledgments

We thank Claudio Gualerzi for strains overproducing initiation factors and for mRNA constructs, Yuri Semenkov and Vladimir Katunin for tRNA preparations, and Petra Striebeck for expert technical assistance. We acknowledge the support of Michael Schatz and Ralf Schmidt (Image Science GmbH) with the IMAGIC software and the contribution of Monika Golas and Bjoern Sander to the EM work with the post(fus) complex. The work was supported by the Deutsche Forschungsgemeinschaft (Wi 626/16-1), the European Commission (BIO4-CT97-2188), the Alfried Krupp von Bohlen und Halbach-Stiftung, and the Fonds der Chemischen Industrie. The CM200 electron microscope was purchased with support of the BBSRC/HEFCE Joint Research Equipment Initiative (grant JREI-97-8010).

Received July 19, 1999; revised December 27, 1999.

References

Ævarsson, A., Brazhnikov, E., Garber, M., Zheltonosova, J., Chirgadze, al-Karadaghi, S., Svensson, L.A., and Liljas, A. (1994). Three-dimensional structure of the ribosomal translocase: elongation factor G from *Thermus thermophilus*. EMBO J. *13*, 3669–3677.

Agrawal, R.K., Penczek, P., Grassucci, R.A., and Frank, J. (1998). Visualization of elongation factor G on the *Escherichia coli* 70S ribosome: the mechanism of translocation. Proc. Natl. Acad. Sci. USA *95*, 6134–6138.

Agrawal, R.K., Heagle, A.B., Penczek, P., Grassucci, R.A., and Frank, J. (1999). EF-G-dependent GTP hydrolysis induces translocation accompanied by large conformational changes in the 70S ribosome. Nat. Struct. Biol. *6*, 643–647.

Al-Karadaghi, S., Ævarsson, A., Garber, M., Zheltonosova, J., and Liljas, A. (1996). The structure of elongation factor G in complex with GDP: conformational flexibility and nucleotide exchange. Structure *4*, 555–565.

Ban, N., Nissen, P., Hansen, J., Capel, M., Moore, P.B., and Steitz, T.A. (1999). Placement of protein and RNA structures into a 5 Å-resolution map of the 50S ribosomal subunit. Nature *400*, 841–847.

Bilgin, N., Richter, A.A., Ehrenberg, M., Dahlberg, A.E., and Kurland, C.G. (1990). Ribosomal RNA and protein mutants resistant to spectinomycin. EMBO J. *9*, 735–739.

Borowski, C., Rodnina, M.V., and Wintermeyer, W. (1996). Truncated elongation factor G lacking the G domain promotes translocation of the 3′ end but not of the anticodon domain of peptidyl-tRNA. Proc. Natl. Acad. Sci. USA *93*, 4202–4206.

Brink, M.F., Brink, G., Verbeet, M.P., and de Boer, H.A. (1994). Spectinomycin interacts specifically with the residues G1064 and C1192 in 16S rRNA, thereby potentially freezing this molecule into an inactive conformation. Nucl. Acids Res. *22*, 325–331.

Calogero, R.A., Pon, C.L., Canonaco, M.A., and Gualerzi, C.O. (1988). Selection of the mRNA translation initiation region by *Escherichia coli* ribosomes. Proc. Natl. Acad. Sci. USA *85*, 6427–6431.

Capel, M.S., Engelman, D.M., Freeborn, B.R., Kjeldgaard, M., Langer, J.A., Ramakrishnan, V., Schindler, D.G., Schneider, D.K., Schoenborn, B.P., Sillers, I.Y., et al. (1987). A complete mapping of the proteins in the small ribosomal subunit of *Escherichia coli*. Science *238*, 1403–1406.

Cate, J.H., Yusupov, M.M., Yusupova, G.Z., Earnest, T.N., and Noller, H.F. (1999). X-ray crystal structures of 70S ribosome functional complexes. Science *285*, 2095–2104.

Clemons, W.M., May, J.L.C., Wimberly, B.T., McCutcheon, J.P., Capel, M.S., and Ramakrishnan, V. (1999). Structure of a bacterial 30S ribosomal subunit at 5.5 Å resolution. Nature *400*, 833–840.

Czworkowski, J., Wang, J., Steitz, T.A., and Moore, P.B. (1994). The crystal structure of elongation factor G complexed with GDP, at 2.7 Å resolution. EMBO J. *13*, 3661–3668.

Davies, J., and Davis, B.D. (1968). Misreading of ribonucleic acid code words induced by aminoglycoside antibiotics. The effect of drug concentration. J. Biol. Chem. *243*, 3312–3316.

Davies, C., Gerstner, R.B., Draper, D.E., Ramakrishnan, V., and White, S.W. (1998). The crystal structure of ribosomal protein S4 reveals a two-domain molecule with an extensive RNA-binding surface: one domain shows structural homology to the ETS DNA-binding motif. EMBO J. *17*, 4545–4558.

Gabashvili, I.S., Agrawal, R.K., Grassucci, R., and Frank, J. (1999). Structure and structural variations of the *Escherichia coli* 30 S ribosomal subunit as revealed by three-dimensional cryo–electron microscopy. J. Mol. Biol. *286*, 1285–1291.

Harauz, G., and van Heel, M. (1986). Exact filters for general geometry three-dimentional reconstruction. Optic *73*, 146–156.

Hausner, T.P., Atmadja, J., and Nierhaus, K.H. (1987). Evidence that the G2661 region of 23S rRNA is located at the ribosomal binding sites of both elongation factors. Biochimie *69*, 911–923.

Heilek, G.M., Marusak, R., Meares, C.F., and Noller, H.F. (1995). Directed hydroxyl radical probing of 16S rRNA using Fe(II) tethered to ribosomal protein S4. Proc. Natl. Acad. Sci. USA *92*, 1113–1116.

Lodmell, J.S., and Dahlberg, A.E. (1997). A conformational switch in *Escherichia coli* 16S ribosomal RNA during decoding of messenger RNA. Science *277*, 1262–1267.

Moazed, D., and Noller, H.F. (1986). Transfer RNA shields specific nucleotides in 16S ribosomal RNA from attack by chemical probes. Cell *47*, 985–994.

Moazed, D., and Noller, H.F. (1987). Chloramphenicol, erythromycin, carbomycin and vernamycin B protect overlapping sites in the peptidyl transferase region of 23S ribosomal RNA. Biochimie *69*, 879–884.

Moazed, D., Robertson, J.M., and Noller, H.F. (1988). Interaction of elongation factors EF-G and EF-Tu with a conserved loop in 23S RNA. Nature *334*, 362–364.

Modolell, J., and Vazquez, D. (1977). The inhibition of ribosomal translocation by viomycin. Eur. J. Biochem. *81*, 491–497.

Mueller, F., and Brimacombe, R. (1997a). A new model for the three-dimensional folding of *Escherichia coli* 16 S ribosomal RNA. I. Fitting the RNA to a 3D electron microscopic map at 20 Å. J. Mol. Biol. *271*, 524–544.

Mueller, F., and Brimacombe, R. (1997b). A new model for the three-dimensional folding of *Escherichia coli* 16 S ribosomal RNA. II. The RNA-protein interaction data. J. Mol. Biol. *271*, 545–565.

Munishkin, A., and Wool, I.G. (1997). The ribosome-in-pieces: binding of elongation factor EF-G to oligoribonucleotides that mimic the sarcin/ricin and thiostrepton domains of 23S ribosomal RNA. Proc. Natl. Acad. Sci. USA *94*, 12280–12284.

Nissen, P., Kjeldgaard, M., Thirup, S., Polekhina, G., Reshetnikova, L., Clark, B.F., and Nyborg, J. (1995). Crystal structure of the ternary complex of Phe-tRNA^{Phe}, EF-Tu, and a GTP analog. Science *270*, 1464–1472.

Noller, H.F., Green, R., Heilek, G., Hoffarth, V., Huttenhofer, A., Joseph, S., Lee, I., Lieberman, K., Mankin, A., and Merryman, C. (1995). Structure and function of ribosomal RNA. Biochem. Cell Biol. *73*, 997–1009.

O'Connor, M., Brunelli, C.A., Firpo, M.A., Gregory, S.T., Lieberman, K.R., Lodmell, J.S., Moine, H., Van Ryk, D.I., and Dahlberg, A.E. (1995). Genetic probes of ribosomal RNA function. Biochem. Cell Biol. *73*, 859–868.

Oleinikov, A.V., Jokhadze, G.G., and Traut, R.R. (1998). A single-headed dimer of *Escherichia coli* ribosomal protein L7/L12 supports protein synthesis. Proc. Natl. Acad. Sci. USA *95*, 4215–4218.

Powers, T., and Noller, H.F. (1991). A functional pseudoknot in 16S ribosomal RNA. EMBO J. *10*, 2203–2214.

Powers, T., and Noller, H.F. (1994). Selective perturbation of G530 of 16 S rRNA by translational miscoding agents and a streptomycin-dependence mutation in protein S12. J. Mol. Biol. *235*, 156–172.

Powers, T., and Noller, H.F. (1995). Hydroxyl radical footprinting of ribosomal proteins on 16S rRNA. RNA *1*, 194–209.

Ramakrishnan, V., and White, S.W. (1992). The structure of ribosomal protein S5 reveals sites of interaction with 16S rRNA. Nature *358*, 768–771.

Rodnina, M.V., and Wintermeyer, W. (1995). GTP consumption of elongation factor Tu during translation of heteropolymeric mRNAs. Proc. Natl. Acad. Sci. USA *92*, 1945–1949.

Rodnina, M.V., Semenkov, Y.P., and Wintermeyer, W. (1994). Purification of fMet-tRNA(fMet) by fast protein liquid chromatography. Ann. Biochem. *219*, 380–381.

Rodnina, M.V., Savelsbergh, A., Katunin, V.I., and Wintermeyer, W. (1997). Hydrolysis of GTP by elongation factor G drives tRNA movement on the ribosome. Nature *385*, 37–41.

Rodnina, M.V., Savelsbergh, A., Matassova, N.B., Katunin, V.I., Semenkov, Y.P., and Wintermeyer, W. (1999). Thiostrepton inhibits turnover but not GTP hydrolysis by elongation factor G on the ribosome. Proc. Natl. Acad. Sci. USA *96*, 9586–9590.

Savelsbergh, A., Mohr, D., Wintermeyer, W., and Rodnina, M.V. (2000). Ribosomal protein L7/12 stimulates GTP hydrolysis on elongation factor G by an RGS-type mechanism. J. Biol. Chem., in press.

Sigmund, C.D., Ettayebi, M., and Morgan, E.A. (1984). Antibiotic resistance mutations in 16S and 23S ribosomal RNA genes of *Escherichia coli*. Nucl. Acids Res. *12*, 4653–4663.

Sköld, S.E. (1983). Chemical crosslinking of elongation factor G to the 23S RNA in 70S ribosomes from *Escherichia coli*. Nucl. Acids Res. *11*, 4923–4932.

Spirin, A.S. (1985). Ribosomal translocation: facts and models. Prog. Nucleic Acid Res. Mol. Biol. *32*, 75–114.

Stark, H., Orlova, E.V., Rinke-Appel, J., Jünke, N., Mueller, F., Rodnina, M.V., Wintermeyer, W., Brimacombe, R., and van Heel, M. (1997a). Arrangement of tRNAs in pre- and posttranslocational ribosomes revealed by electron cryomicroscopy. Cell *88*, 19–28.

Stark, H., Rodnina, M.V., Rinke-Appel, J., Brimacombe, R., Wintermeyer, W., and van Heel, M. (1997b). Visualization of elongation factor Tu on the *Escherichia coli* ribosome. Nature *389*, 403–406.

van Heel, M. (1987). Angular reconstruction: a posteriori assignment of projection directions for 3-D reconstruction. Ultramicroscopy *21*, 111–124.

VanLoock, M.S., Easterwood, T.R., and Harvey, S.C. (1999). Major groove binding of the tRNA/mRNA complex to the 16S ribosomal RNA decoding center. J. Mol. Biol. *285*, 2069–2078.

Wilson, K.S., and Noller, H.F. (1998). Mapping the position of translational elongation factor EF-G in the ribosome by directed hydroxyl radical probing. Cell *92*, 131–139.